Ionization by strong circularly polarized fields

Ingo Dreißigacker, Jost Henkel, Ingo Barth, Manfred Lein

August 2014

Outline

Ionization by strong circularly polarized fields

- The transverse width of electron momentum distributions
- Molecular imaging from 3D momentum distributions
- Photoelectron circular dichroism
- Dependence on bound-state angular momentum

The transverse momentum distribution

Transverse momentum distribution

Momentum distribution in the direction orthogonal to the applied strong field

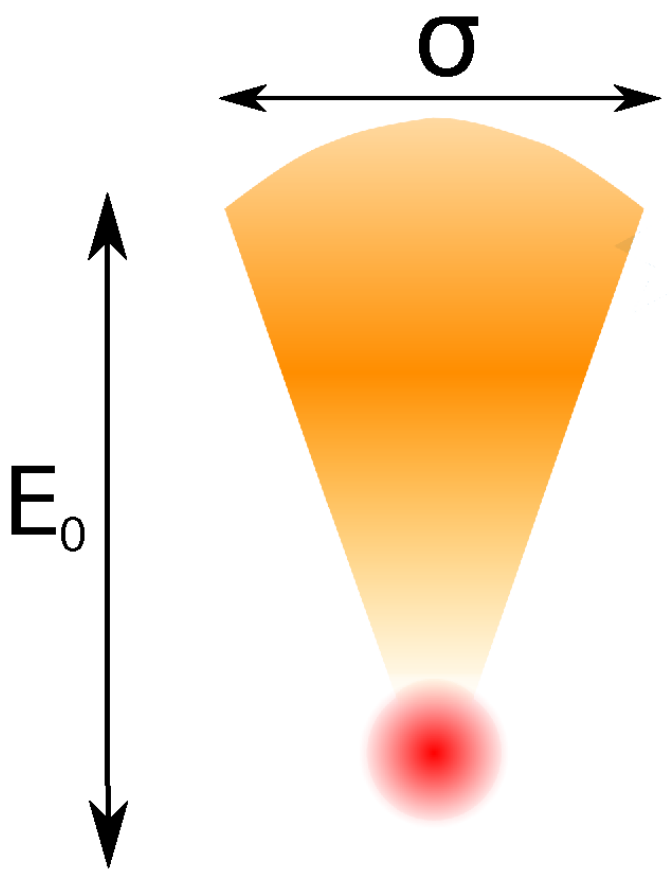

Experiments

Measured widths of transverse distributions (circularly polarized light)

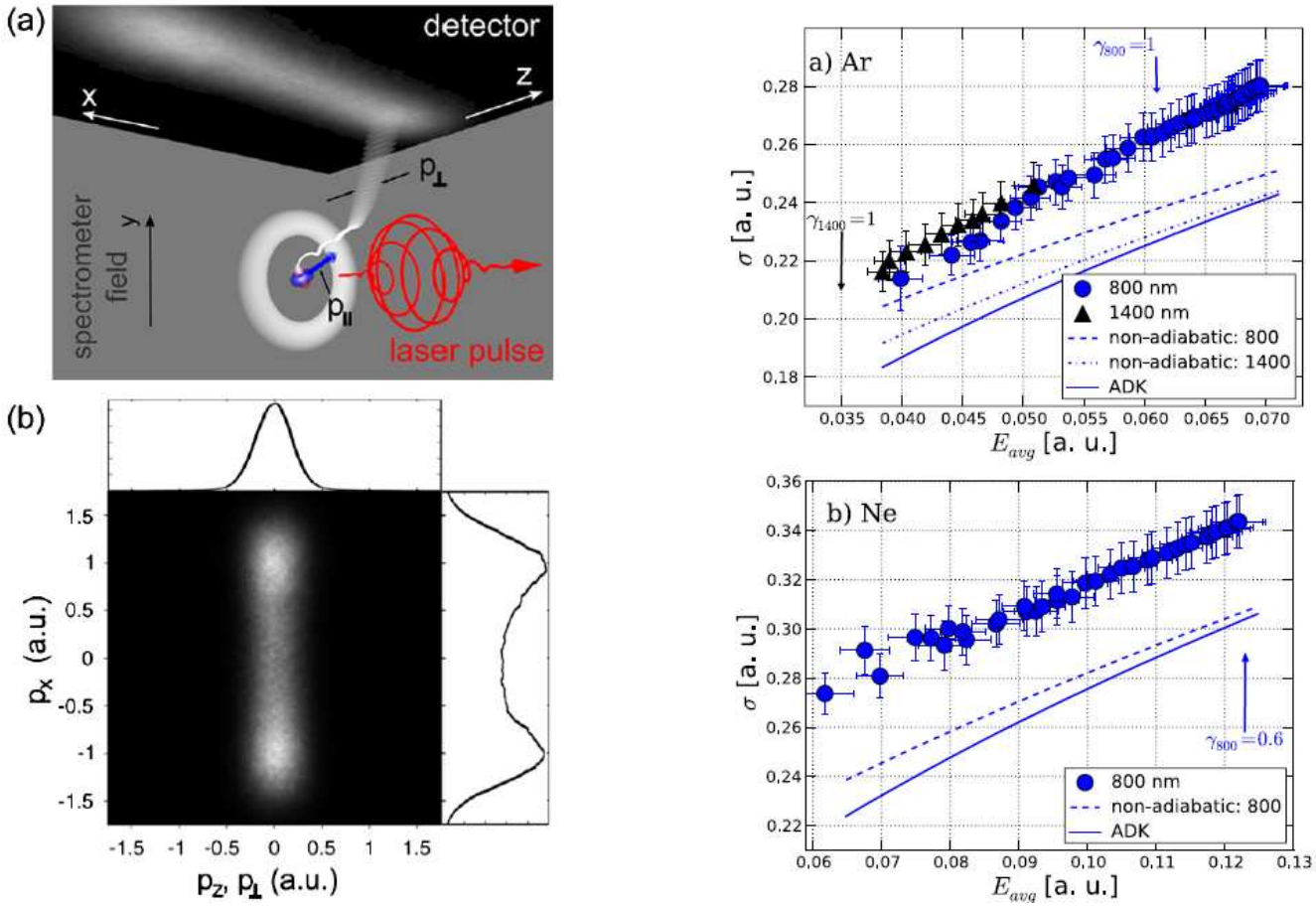

Arissian et al., PRL 105, 133002 (2010)

→ Widths are larger than predicted by a simple tunnelling formula

$$|\Psi(k_\perp)|^2 = |\Psi_0(k_\perp)|^2 \exp(-k_\perp^2 \sqrt{2I_p}/E).$$

Experiments

Transverse distribution from linearly polarized fields is more complicated due to Coulomb effects:

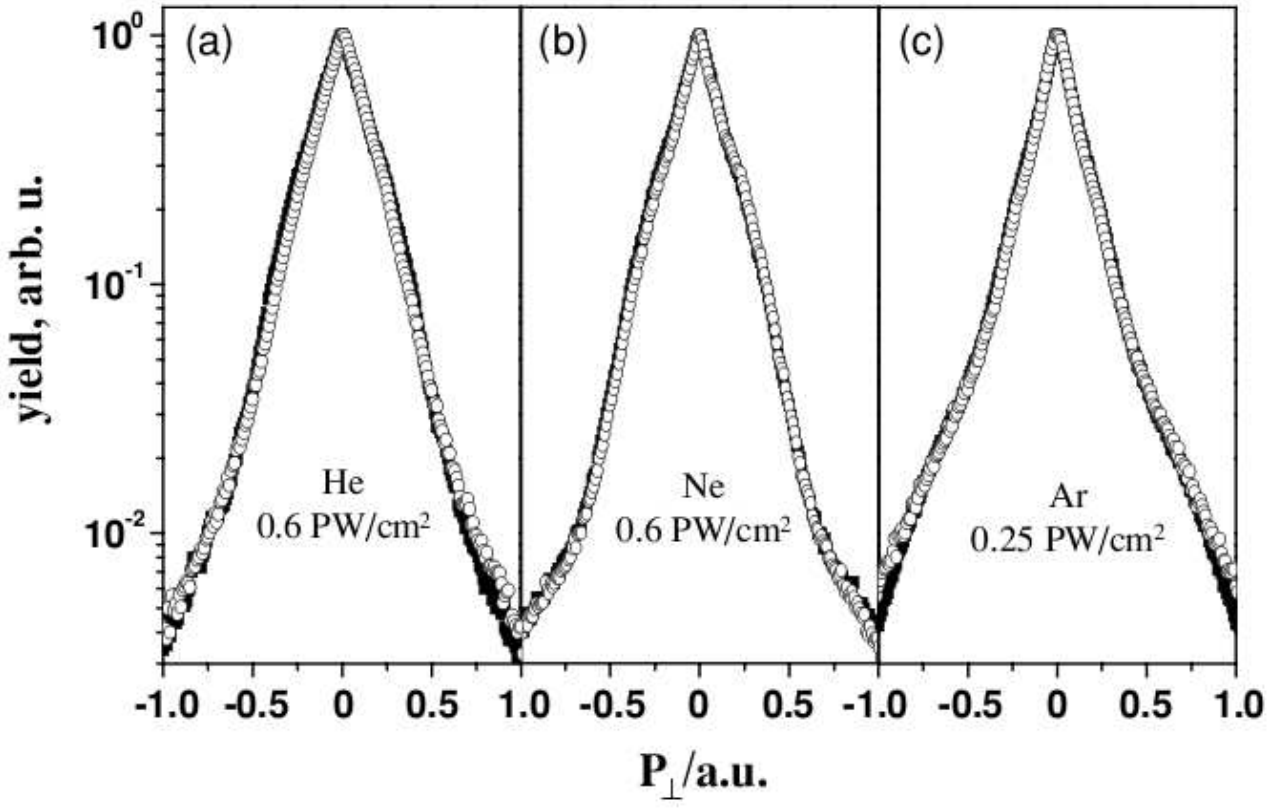

Rudenko et al., J. Phys. B 38, L191 (2005)

Tunnelling theory of the transverse distribution

Quick derivation:

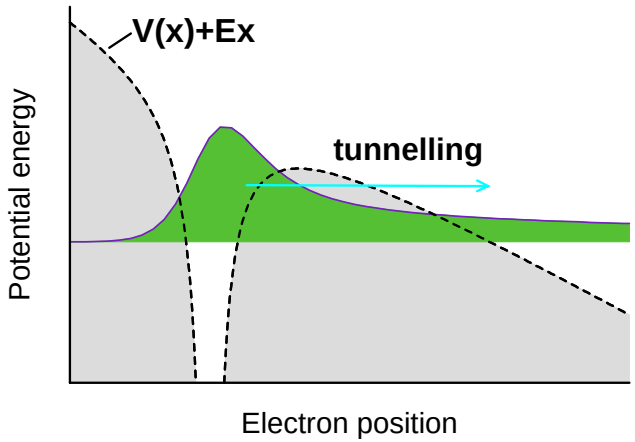

Recall tunnelling formula for ionization rate

$$\boxed{\Gamma \propto e^{-2(2I_\mathrm{p})^{3/2}/(3E)}}$$ with $E =$ electric field (Landau/Lifshitz).

If electron has transverse momentum $k_\perp$, then $k_\perp^2/2$ less energy is available for pushing against the barrier.

$$\rightarrow \Gamma \propto e^{-2(2I_\mathrm{p}+k_\perp^2)^{3/2}/(3E)} \overrightarrow{\text{Taylor}} e^{-2(2I_\mathrm{p})^{3/2}/(3E)}\, e^{-k_\perp^2\sqrt{2I_\mathrm{p}}/E}$$

$\rightarrow$ Simple estimate for the transverse width: $\sigma \sim \sqrt{E/\sqrt{2I_\mathrm{p}}}$.

Tunnelling theory of the transverse distribution

Prefactor

- Heuristic choice: bound-state momentum distribution
- Systematic derivation: by saddle-point approximation / strong-field approximation (SFA)

SFA: $$M(\mathbf{k}) = -i \int_{t_0}^{t_f} \mathrm{d}t \, \langle \mathbf{k} + \mathbf{A}(t) | \mathbf{r} \cdot \mathbf{E}(t) | \psi_0 \rangle \, e^{iS(\mathbf{k},t)}$$ [Keldysh, Faisal,Reiss]

with plane-wave states $|\mathbf{k} + \mathbf{A}(t)\rangle$, action

$$S(\mathbf{k}, t) = \int^{t} \mathrm{d}t' \, [I_p + (\mathbf{k} + \mathbf{A}(t'))^2/2].$$

and $\mathbf{A}(t) = \int^t E(t')dt'$.
Saddle-point approximation: $M(\mathbf{k}) = \sum_{t_s} C(\mathbf{p}, t_s) \exp(iS(\mathbf{k}, t))$
with saddle-point times t_s satisfying $(\mathbf{k} + \mathbf{A}(t_s))^2/(2m) = -I_\mathrm{p}$.

Tunnelling theory of the transverse distribution

SFA: $M(\mathbf{k}) = -i \int_{t_0}^{t_f} \mathrm{d}t\, D(\mathbf{k},t)\, e^{iS(\mathbf{k},t)}$ with $D(\mathbf{k},t) = \langle \mathbf{k}+\mathbf{A}(t)|\mathbf{r}\cdot\mathbf{E}(t)|\psi_0\rangle$

Saddle-point condition: $\dot{S}(\mathbf{k},t_s) = 0$ gives complex t_s.

Complication: $D(\mathbf{k},t)$ has a pole at t_s.

Result for pole of order q, with $\tilde{D}(\mathbf{k},t_s) = \lim_{t\to t_s} D(\mathbf{k},t)(t-t_s)^q$, using linear polarization (for simplicity):

$$|M(\mathbf{k})|^2 = 4\pi \left(\frac{\Gamma(q/2)}{2\Gamma(q)}\right)^2 |2\,(\mathbf{k}+\mathbf{A}(t_s))\cdot\mathbf{E}(t_s)|^{q-1} \times |\tilde{D}(\mathbf{k},t_s)|^2\, |\exp(i\,S(\mathbf{k},t_s))|^2 .$$

(quantitative tunnelling formula QTF)

Provides analytical formula for analytical bound-state orbitals.

Application to half-cycle pulses acting on:

- hydrogen atom with exact 1s ground state
- Ne and Ar with hydrogenlike 2p and 3p orbitals, effective Z

Results: hydrogen atom

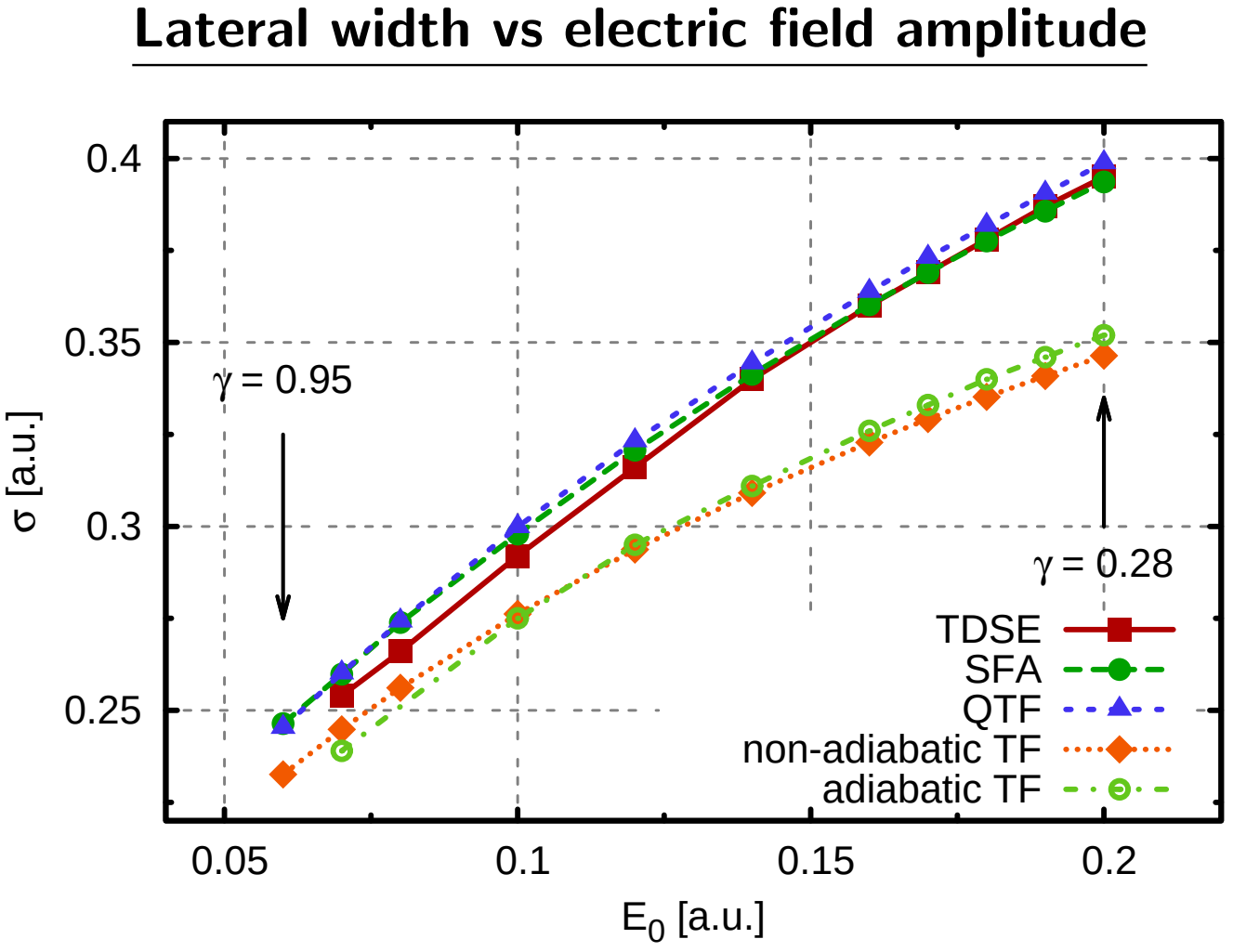

I. Dreissigacker and M.L., Chem. Phys. 414, 69 (2013)

Excellent agreement between TDSE / SFA / QTF

Results: Ar and Ne

Transverse width vs electric field amplitude

Ar

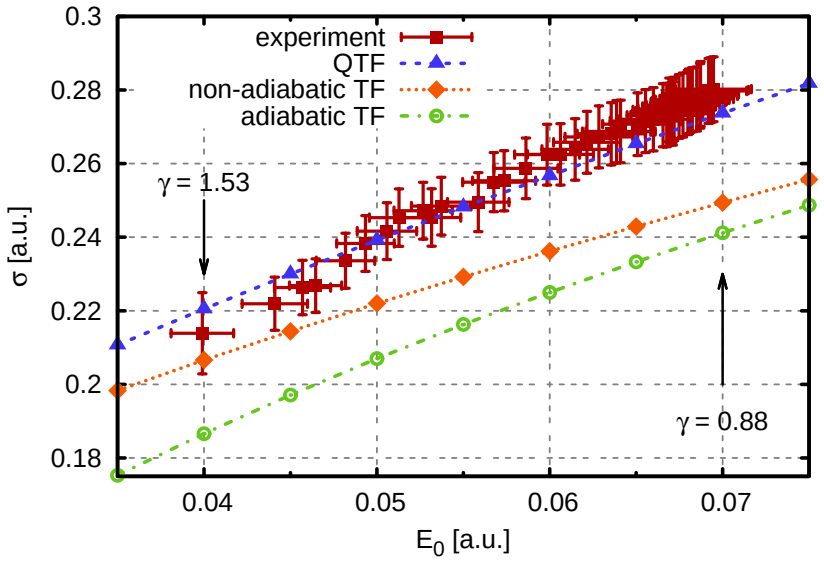

Ne

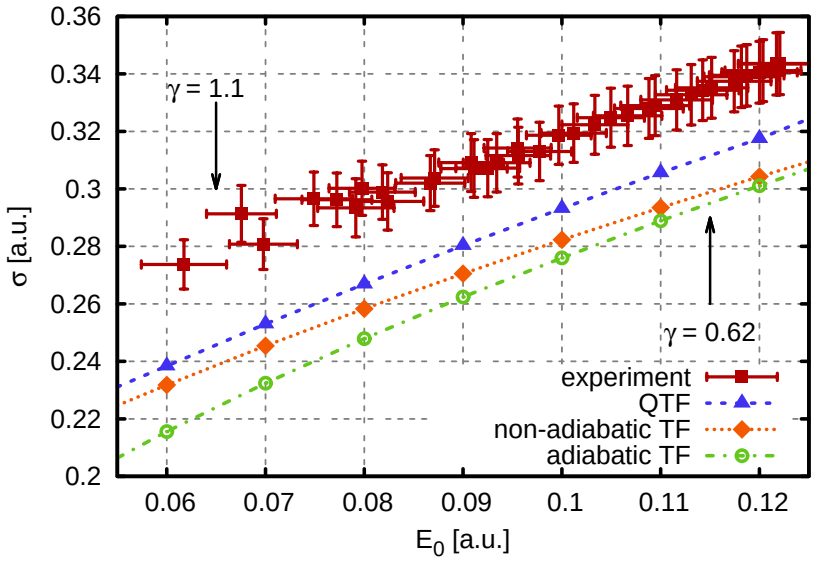

I. Dreissigacker and M.L., Chem. Phys. 414, 69 (2013)

→ Excellent agreement for Ar

Remaining deviation for Ne.

Reason seems beyond single-active-electron theory.

Time-dependent Schrödinger equation (TDSE)

Two types of 3-dimensional TDSE calculations

CP: Circularly polarized three-cycle pulses, 3D cartesian grid,
atom with soft-core potential $-1/\sqrt{r^2+0.2}$, $I_p = 0.364$ a.u.,
Fourier split-operator method

LP: Linearly polarized half-cycle pulses, cylindrical grid, $-1/r$ potential,
Hankel-Fourier split-operator method

Solve TDSE for atom plus field (*wavelength 800 nm*),

$$i\frac{\partial\Psi(t)}{\partial t} = H\Psi(t)$$

and calculate momentum distributions of outgoing electrons, either on a large grid or by projection on plane waves and collection in an outer grid.

Results

Momentum distributions for circularly polarized pulses, projected into the polarization plane (dashed: classical $\mathbf{p} = -\mathbf{A}(t)$)

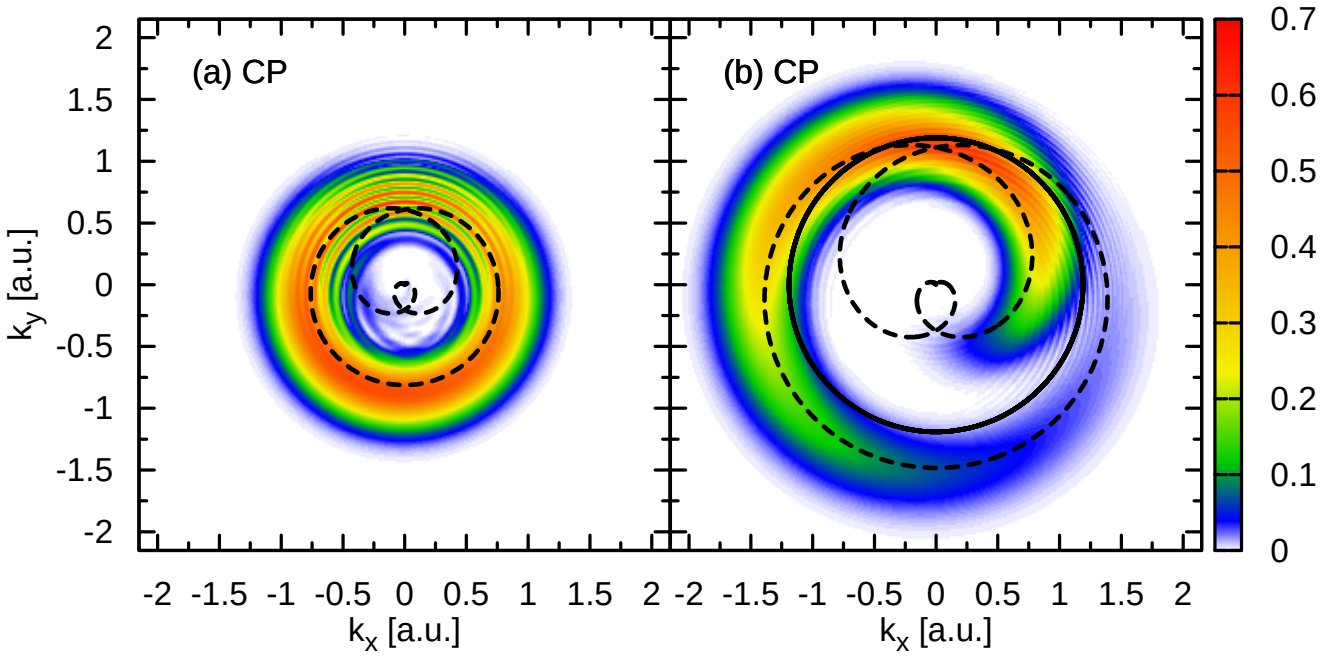

(a) $E_0 = 0.046\mathrm{a.u.}$ (b) $E_0 = 0.084\mathrm{a.u.}$

Henkel et al., PRA 85, 021402(R) (2012)

low intensity: maximum emission at approx. maximum field
high intensity: angle of maximum emission shifts due to depletion

Results

Widths compared to tunneling model

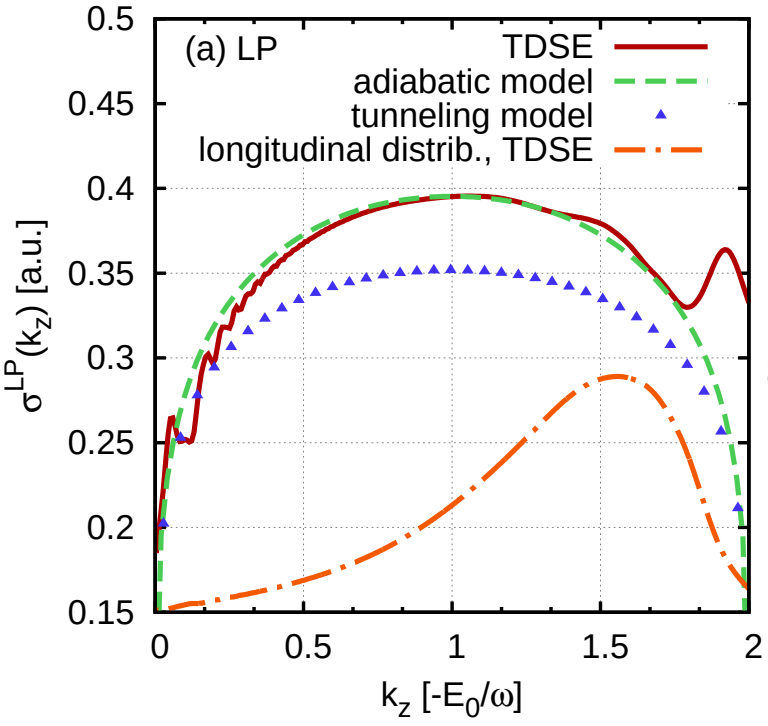

$E_0 = 0.2\,\text{a.u.}$

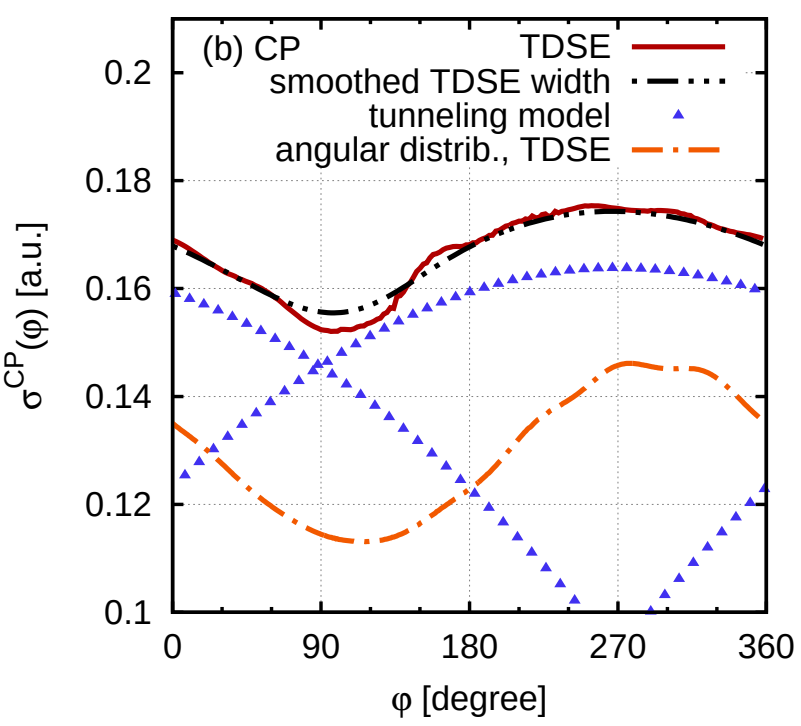

$E_0 = 0.027\,\text{a.u.}$

- Widths follow the instantaneous field on a sub-cycle scale.
- Angle dependence of width shows no "attoclock shift" .

Transverse widths for molecular imaging

Widths are sensitive to

- field strength
- electronic structure (orbital shape)

→ Use circularly polarized field for

- imaging of (aligned) orbitals and
- detection of multiorbital ionization.

[see also
Zhu et al., Opt. Express **19**, 13722 (2011),
Holmegaard et al., Nat. Phys. **6**, 428 (2010)]

TDSE momentum distributions (H_2^+)

- 3D TDSE calculations for an H_2^+ molecular ion aligned along x.
  (Fixed nuclei, soft-core potential close to the exact H_2^+ potential)
- Three-cycle $\sin^2$ circularly polarized pulses at 800 nm,
  $I = 8.5 \times 10^{14}\,\mathrm{W/cm^2}$.
- Vary direction of peak field relative to molecular axis (i.e. vary CEP)

TDSE momentum distributions (H_2^+)

Various directions of peak of vector potential:

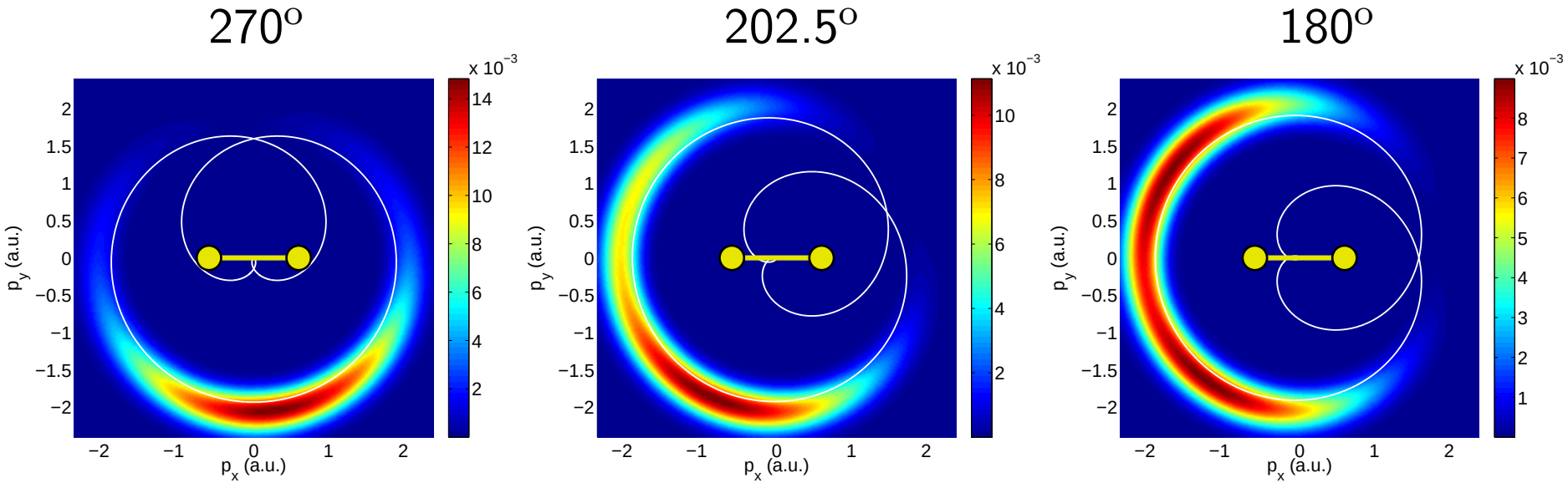

→ Shift of emission angle (cf. attoclock Eckle et al.)

→ Preferential ionization when field is parallel to molecule

→ Double maximum for peak field perpendicular to molecule (180° case)

TDSE angular distribution and transverse widths (H_2^+)

Comparison of TDSE results with cw SFA

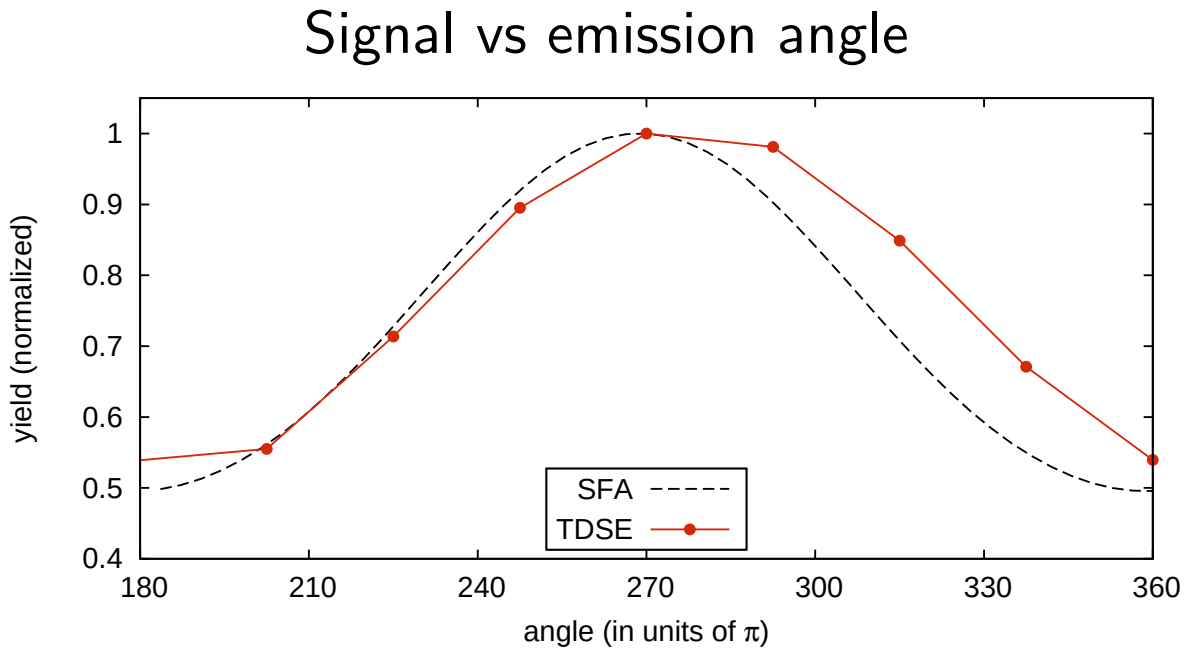

→ Reasonable agreement with SFA.

TDSE angular distribution and transverse widths (H_2^+)

Comparison of TDSE results with cw SFA

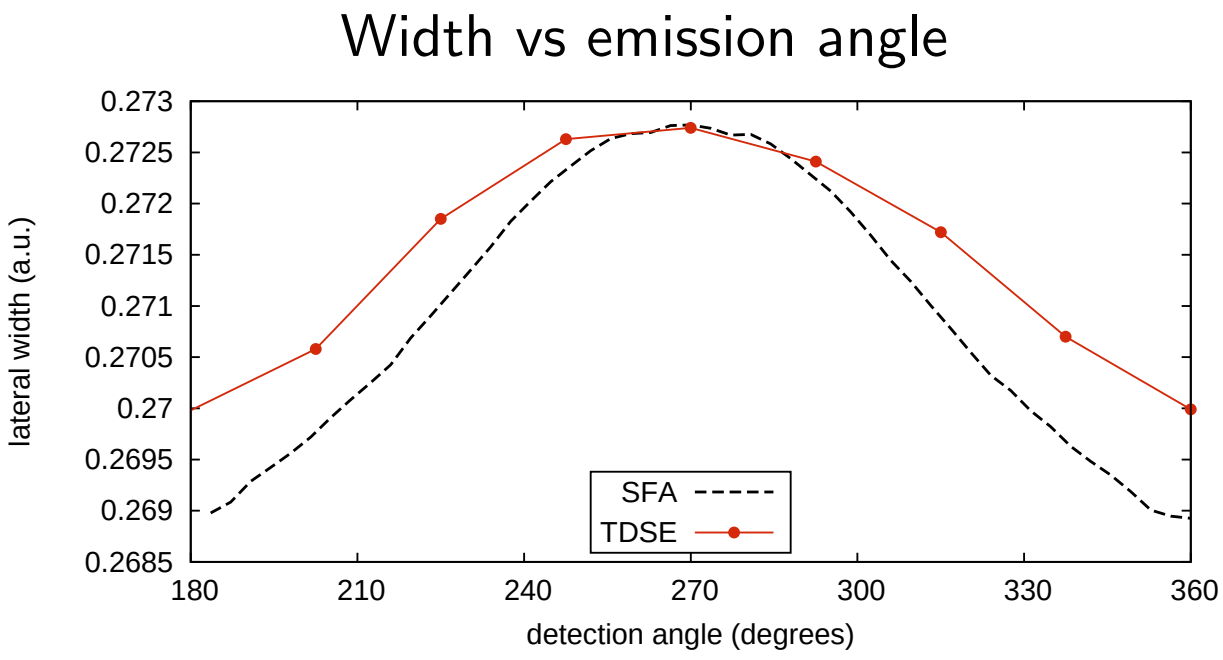

→ Maximum of Width shows little angular shift (no "attoclock effect").

→ SFA gives quantitatively reliable widths

Application to real-world molecules

Assume 1D alignment with molecular axis in the plane of circular polarization.

HOMOs:

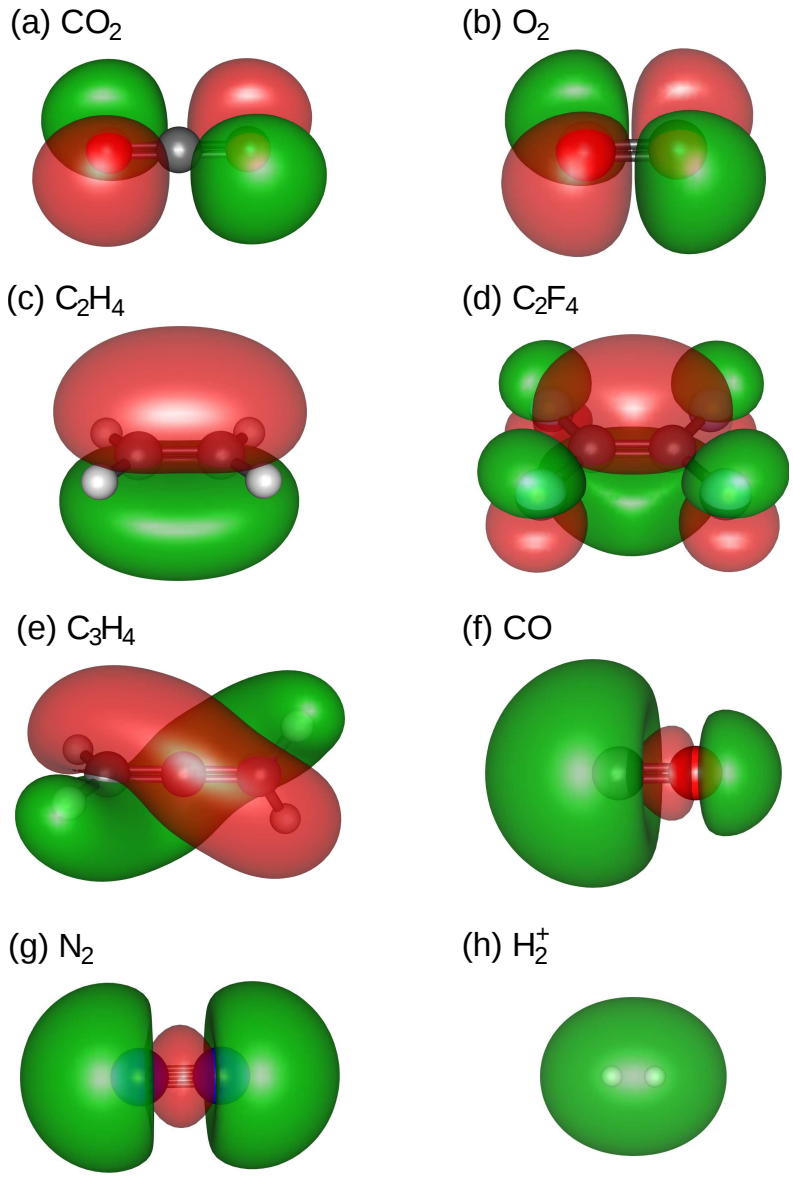

Results: aligned molecules (SFA for circular polarization)

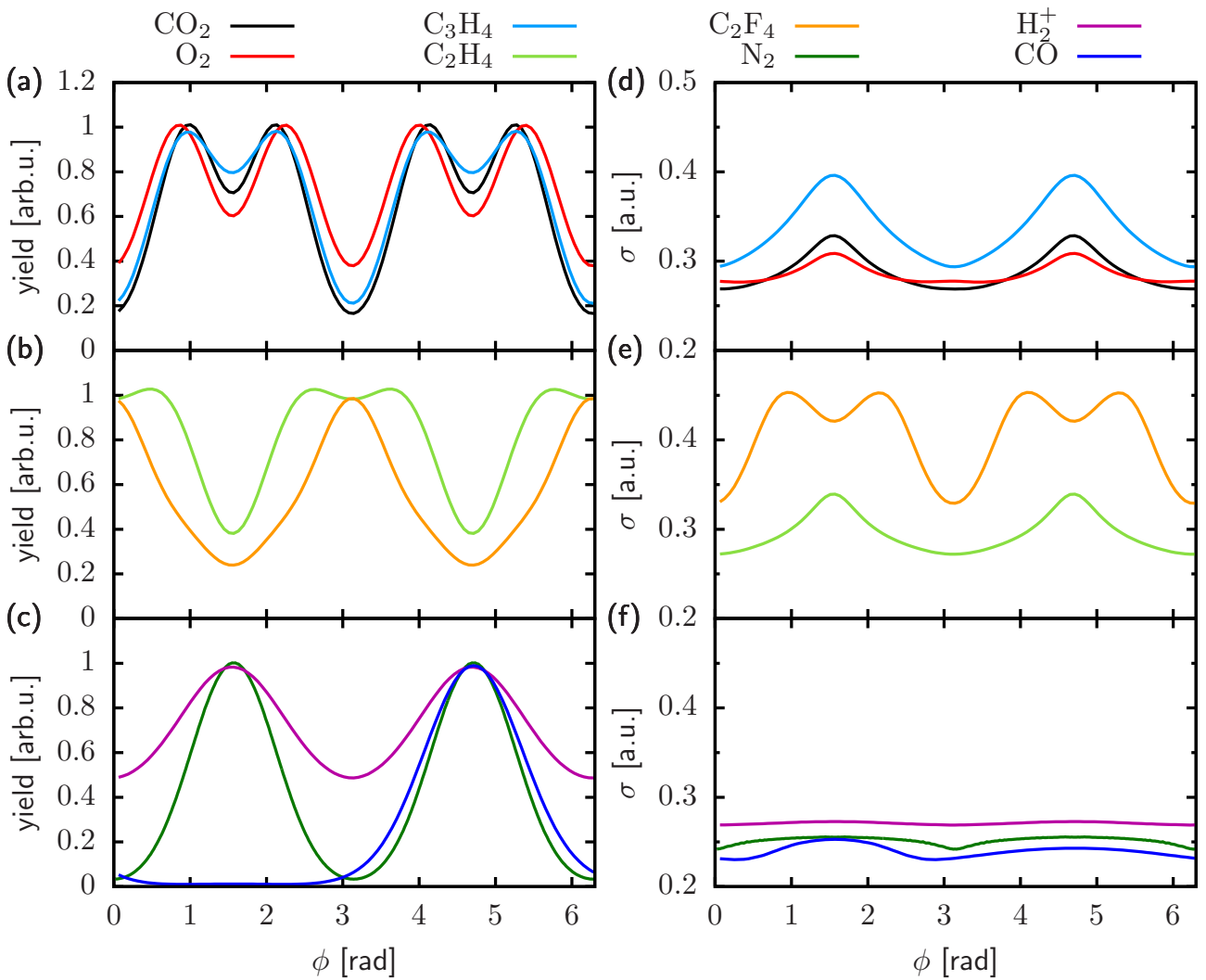

- σ-orbitals (no nodal planes) show little variation of width.
- Strong variations for other cases.

Example: CO_2 with two degenerate HOMOs

Molecular axis in the *xy*-plane (plane of circular polarization)

Transverse distributions vs emission angle

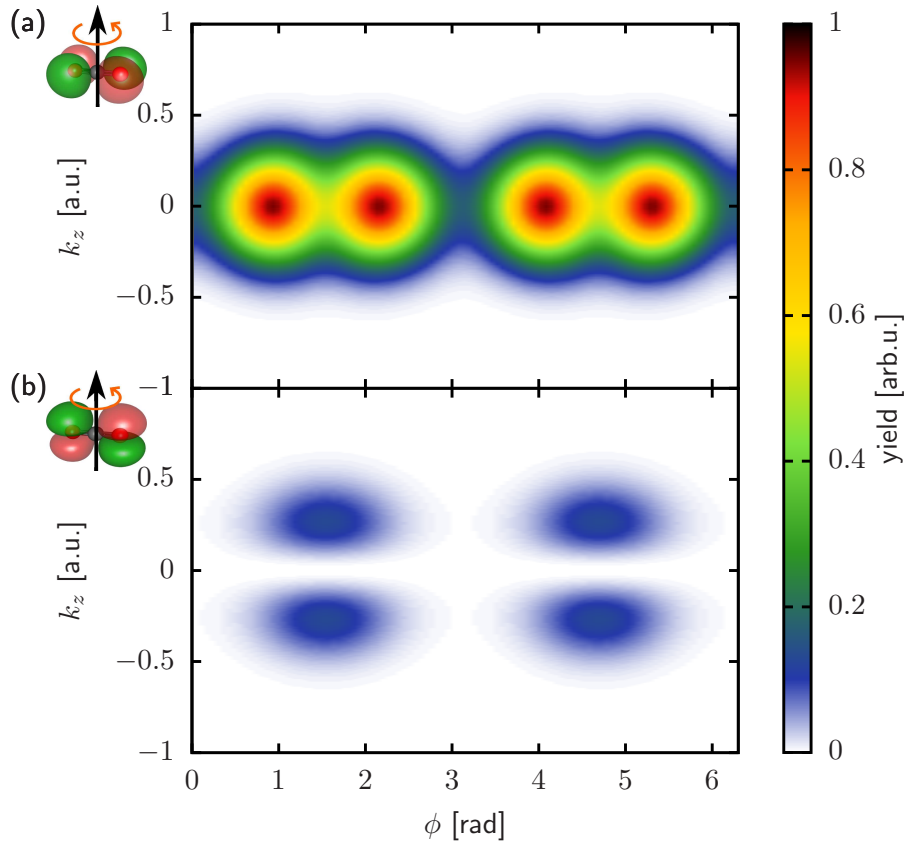

→ Momentum distribution reflects presence of nodal plane.

→ Stronger contribution from orbital "inside" *xy*-plane.

Example: CO_2 with two degenerate HOMOs

Signal and transverse width vs emission angle

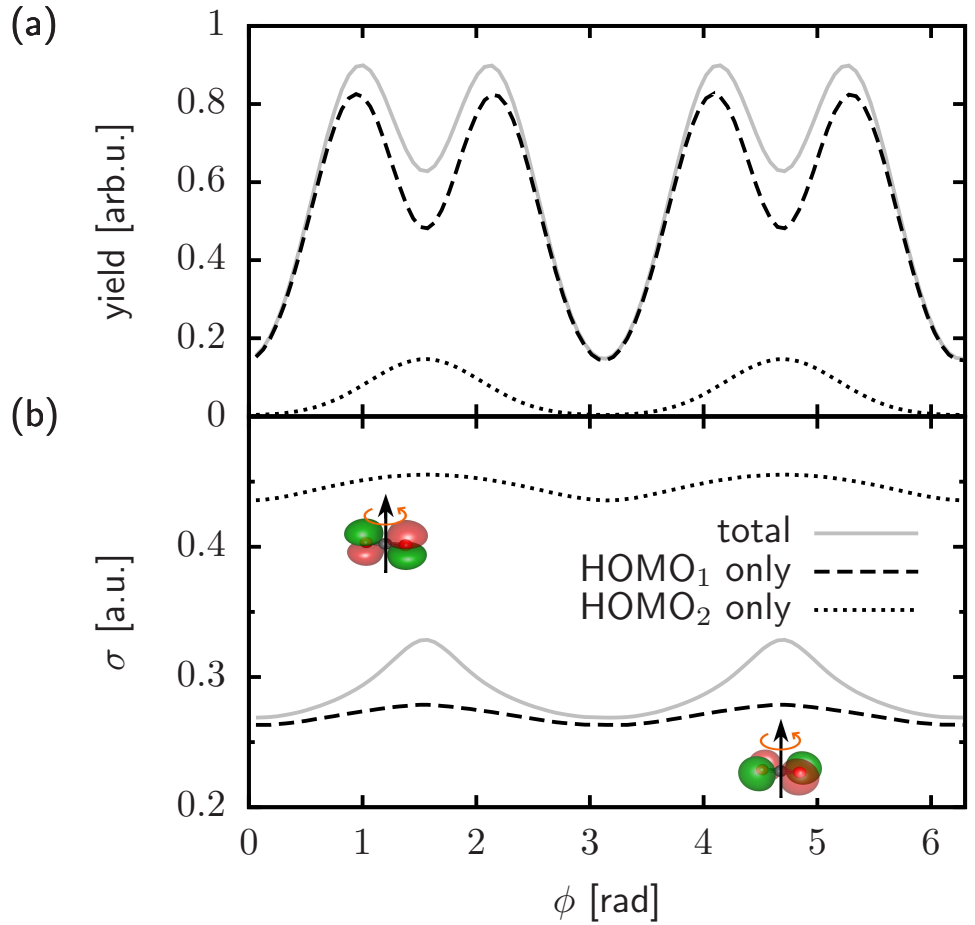

- Strong variation of **signal**/little variation of **width** for individual orbitals.
- Variation in **total width** arises from different weighting.

→ **Width detects multi-orbital contributions.**

Strong-field photoelectron circular dichroism

Strong-field photoelectron circular dichroism

- Ionization of chiral molecules with circularly polarized laser pulses
- Observable: three-dimensional photoelectron distribution
- Search for forward-backward asymmetry

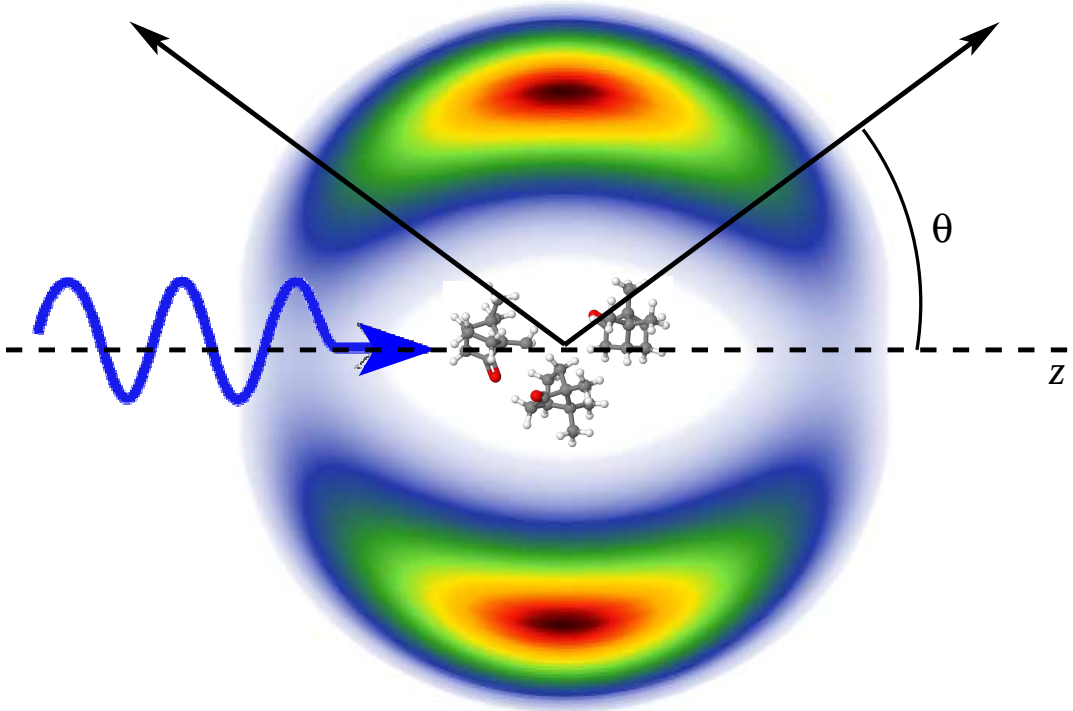

$$I(\theta) = 1 + P_1(\cos\theta)) + P_2(\cos\theta)) + \ldots$$

[Ritchie, PRA 13, 1411 (1976); Cherepkov, CPL 87, 344 (1982); Powis, JCP 112, 301 (2000); Böwering et al., PRL 86, 1187 (2001)]

Strong-field photoelectron circular dichroism

Femtosecond pulse PECD [Lux et al., Angew. Chem. Int. Ed. 51, 5001 (2012)]

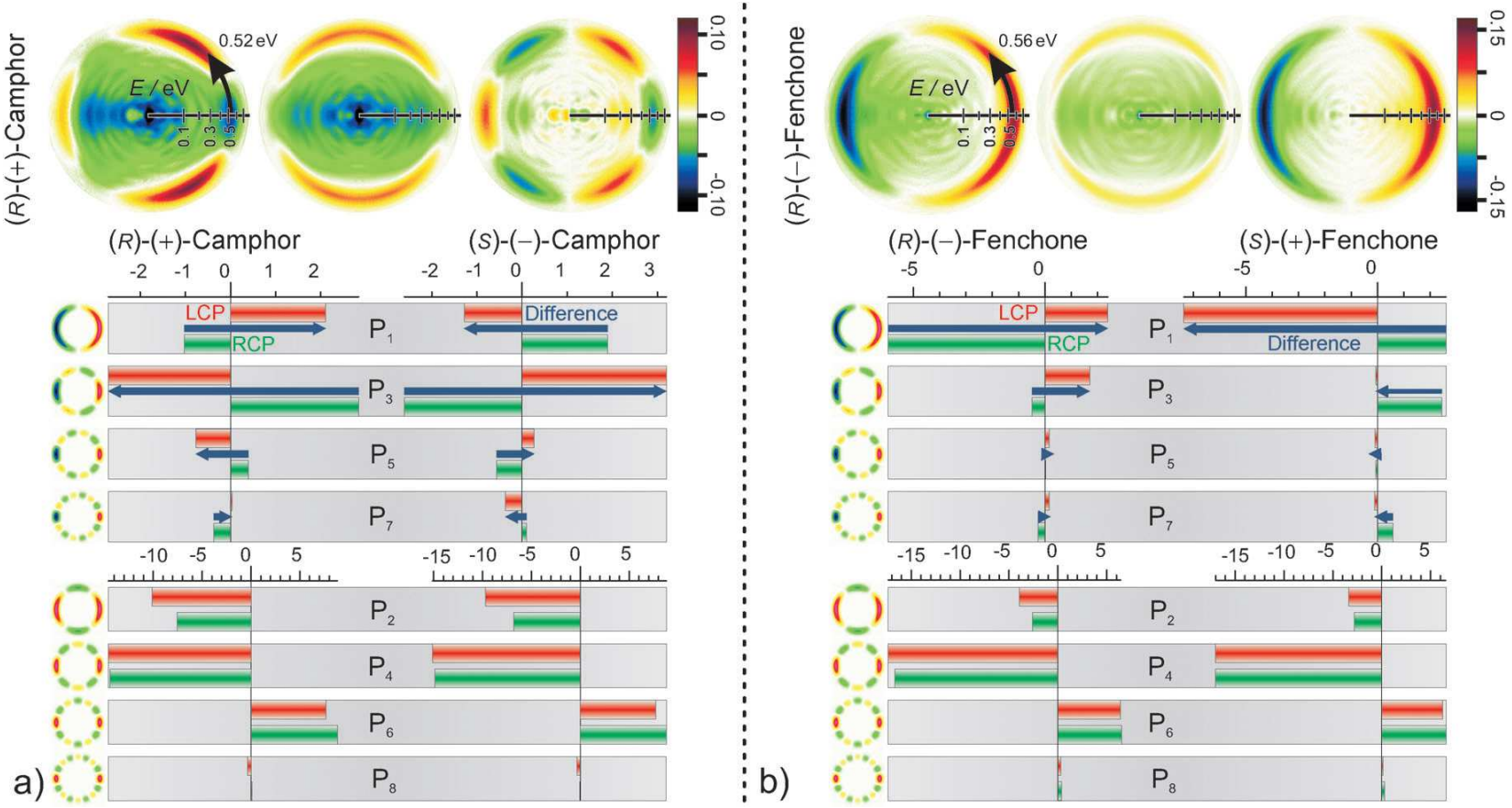

See also: Lehmann et al., JCP **139**, 234307 (2013)

Strong-field approximation for chiral molecules

Conventional SFA: $$M(\mathbf{k}) = -i \int_{t_0}^{t_f} \mathrm{d}t \, \langle \psi^{(-)}_{\mathbf{k}+\mathbf{A}(t)} | \mathbf{r} \cdot \mathbf{E}(t) | \psi_0 \rangle \, e^{iS(\mathbf{k},t)}$$

with $\psi^{(-)}_{\mathbf{k}}$ = plane waves does *not* yield forward-backward asymmetry!

$\rightarrow$

- Use approximate continuum states from the Born approximation:

$$\psi^{(-)}_{\mathbf{k}} = \exp(i\mathbf{k}\cdot\mathbf{r}) - \frac{1}{2\pi} \int d^3r' \frac{\exp(-ik|\mathbf{r}-\mathbf{r}'|)}{|\mathbf{r}-\mathbf{r}'|} V(\mathbf{r}') \exp(i\mathbf{k}\cdot\mathbf{r}')$$

- Obtain bound orbital (HOMO) ψ_0 and potential V from GAUSSIAN.
- Apply to camphor and fenchone ($C_{10}H_{16}O$)
- $\lambda = 398\,\mathrm{nm}$ and $I = 2.5 \times 10^{13}\,\mathrm{W/cm^2}$

Camphor and fenchone HOMOs

R-camphor

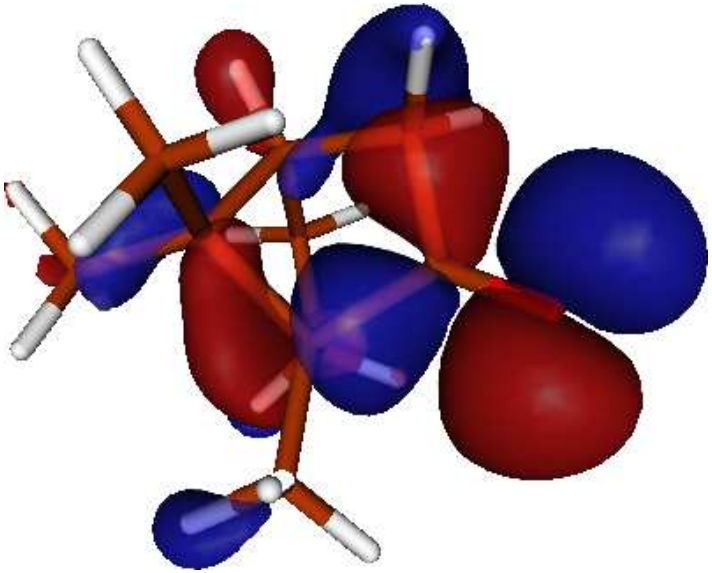

R-fenchone

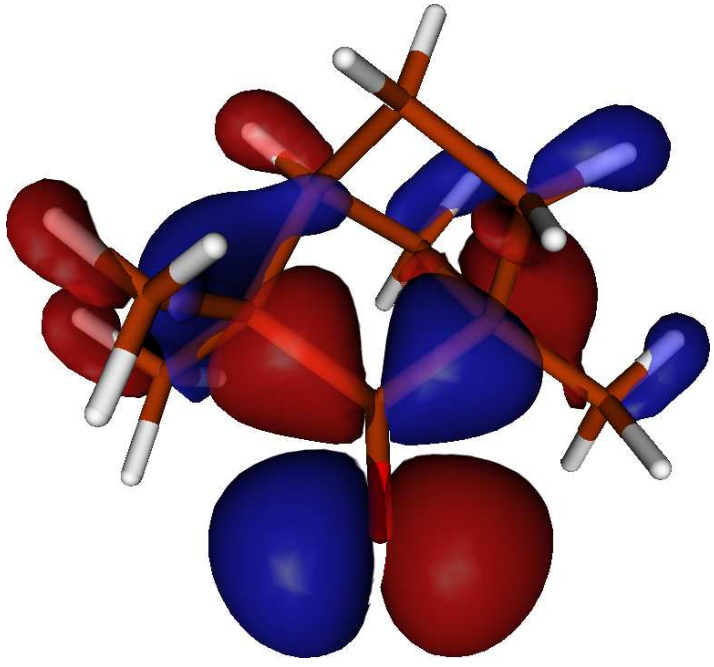

Photoelectron distributions

R-fenchone, single orientation, LCP pulse (total length 20 cycles)

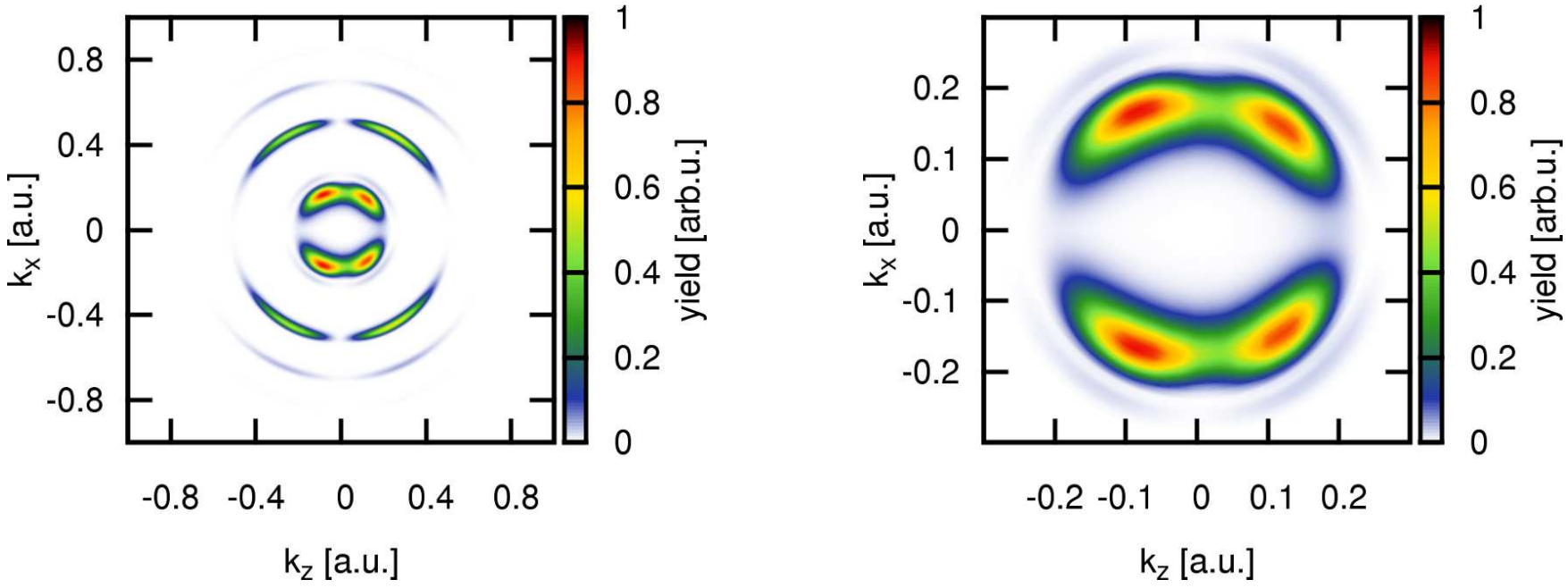

I. Dreissigacker and M.L., PRA 89, 053406 (2014)

- Three-, four- and five-photon rings are visible.
- Asymmetry due to single orientation.

Photoelectron distributions

R-fenchone, random orientation (numerically averaged over Euler angles)

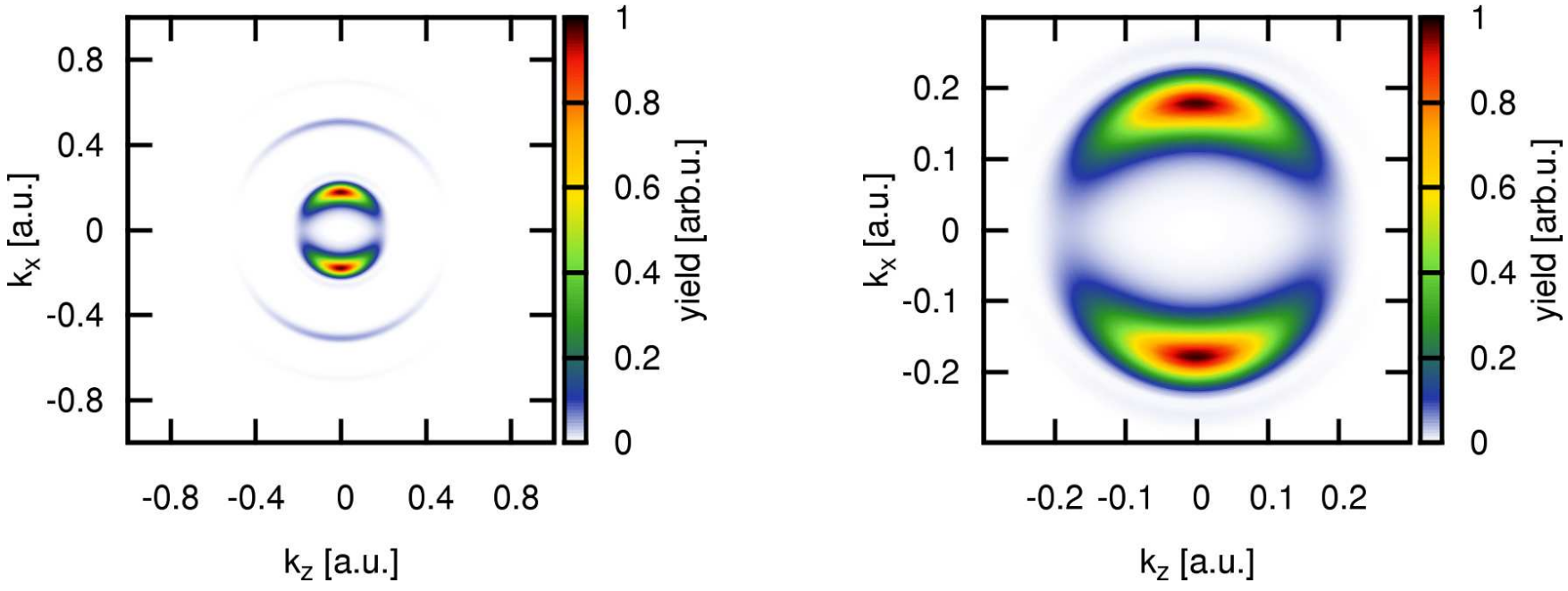

- Asymmetry is reduced by angle averaging.
- Camphor distribution looks practically the same as in fenchone.

Forward-backward asymmetries

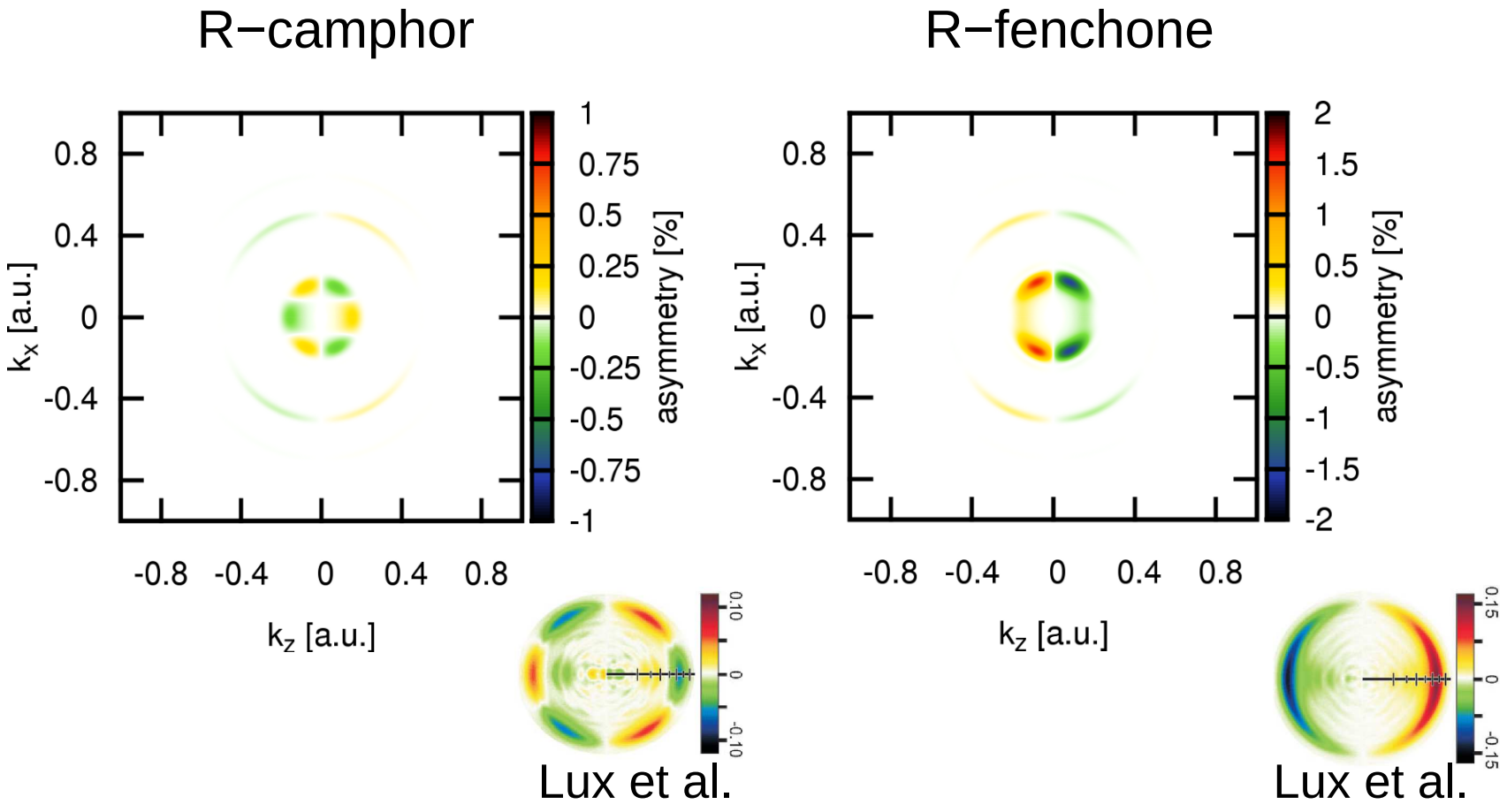

- Nodal structure in good agreement with experiment
- Asymmetries smaller and of different sign compared to experiment
- Fenchone gives stronger asymmetry (matches experiment)

Legendre expansion (odd coefficients)

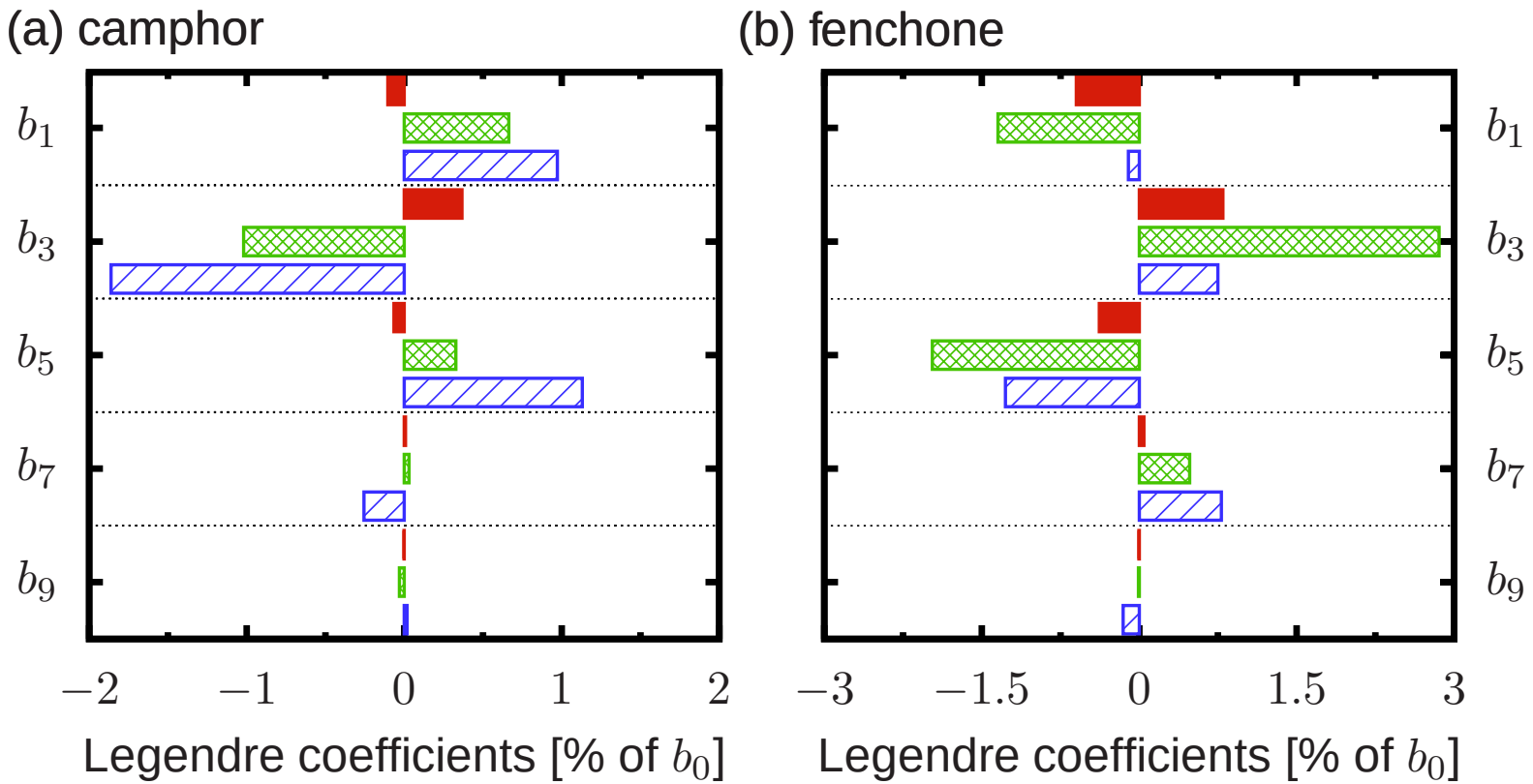

photon numbers: three, four, five

- For camphor, asymmetry increases with photon number
- The sign of asymmetry is mostly independent of the photon number.

Possible issues

Effects not included in the present model:

- Intermediate resonances
- Laser-induced alignment
- Exact continuum treatment

m-dependence of atomic ionization

m-dependence of atomic ionization

Ionization of p-orbitals ($l = 1$) with circular polarization
$\rightarrow$ dependence on m quantum number?

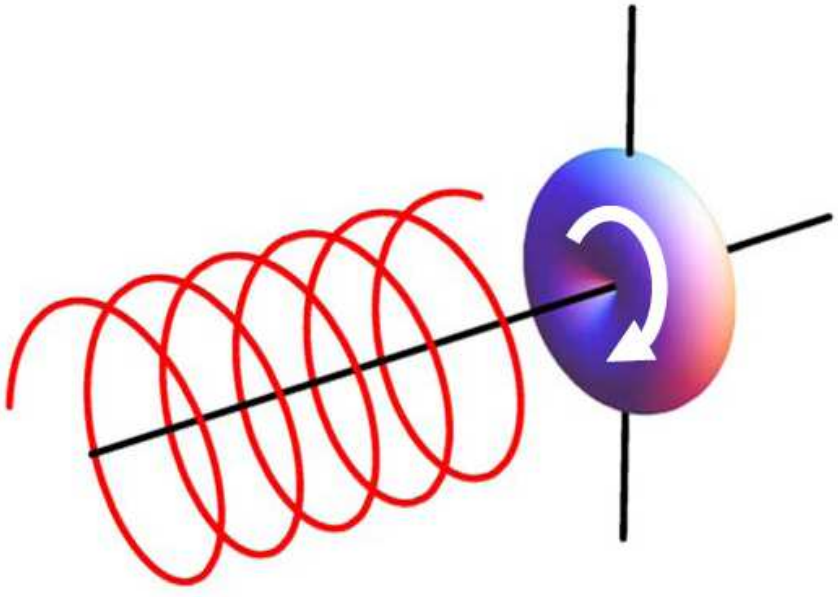

Theory by Barth and Smirnova (PRA 87, 013433 2013)
[see also B. Bergues et al. PRL 95, 263002 (2005)]:

Preferential ionization of counterrotating electrons
$\rightarrow$ Emission of spin-polarized electrons by spin-orbit coupling
[Barth, Smirnova, PRA 88, 013401 (2013)]

m-dependence of atomic ionization

Theory based on Perelomov, Popov and Terent'ev (PPT)

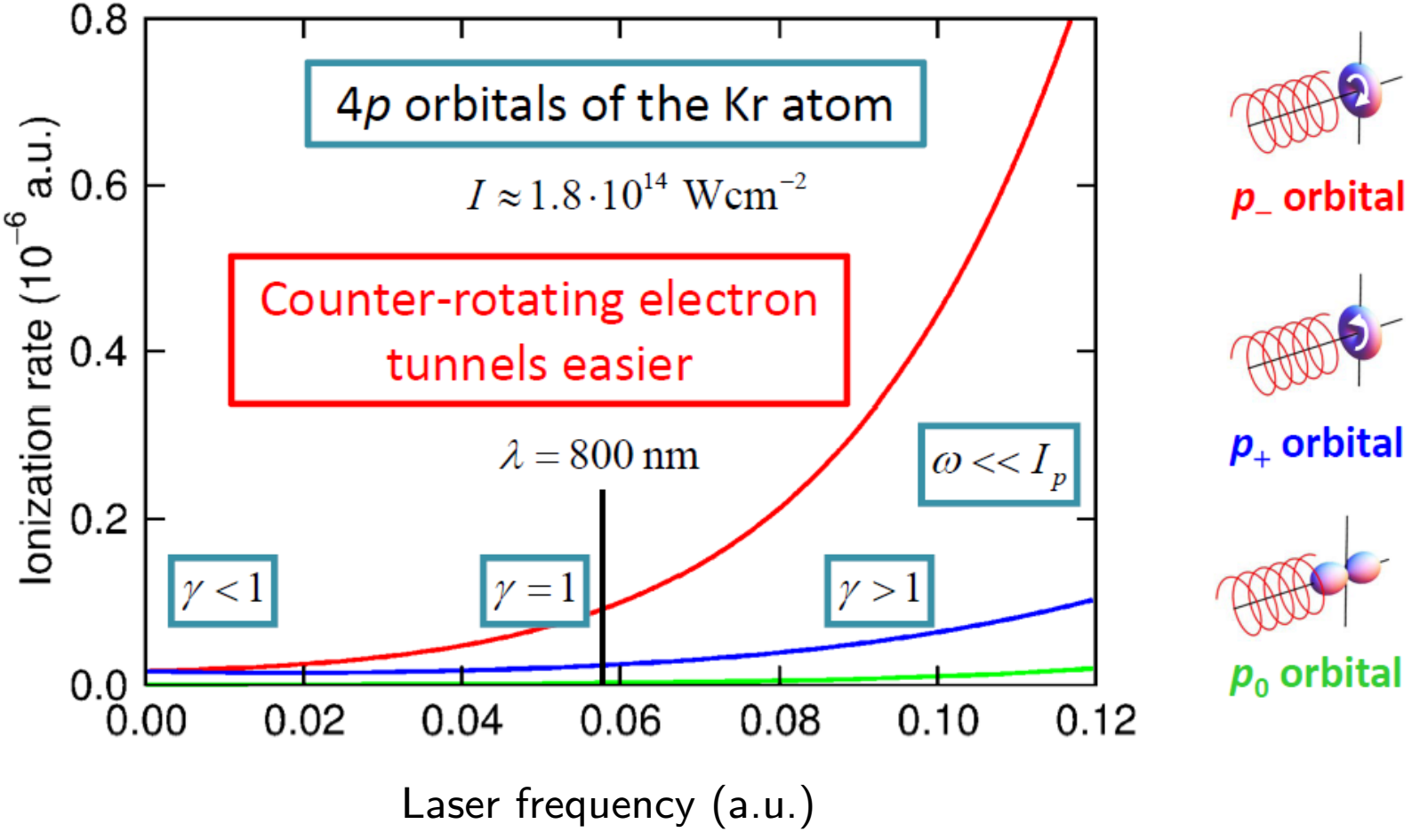

Barth, Smirnova PRA 87, 013433 2013

m-dependence of atomic ionization

Numerical solution of the TDSE for a 2D Neon model

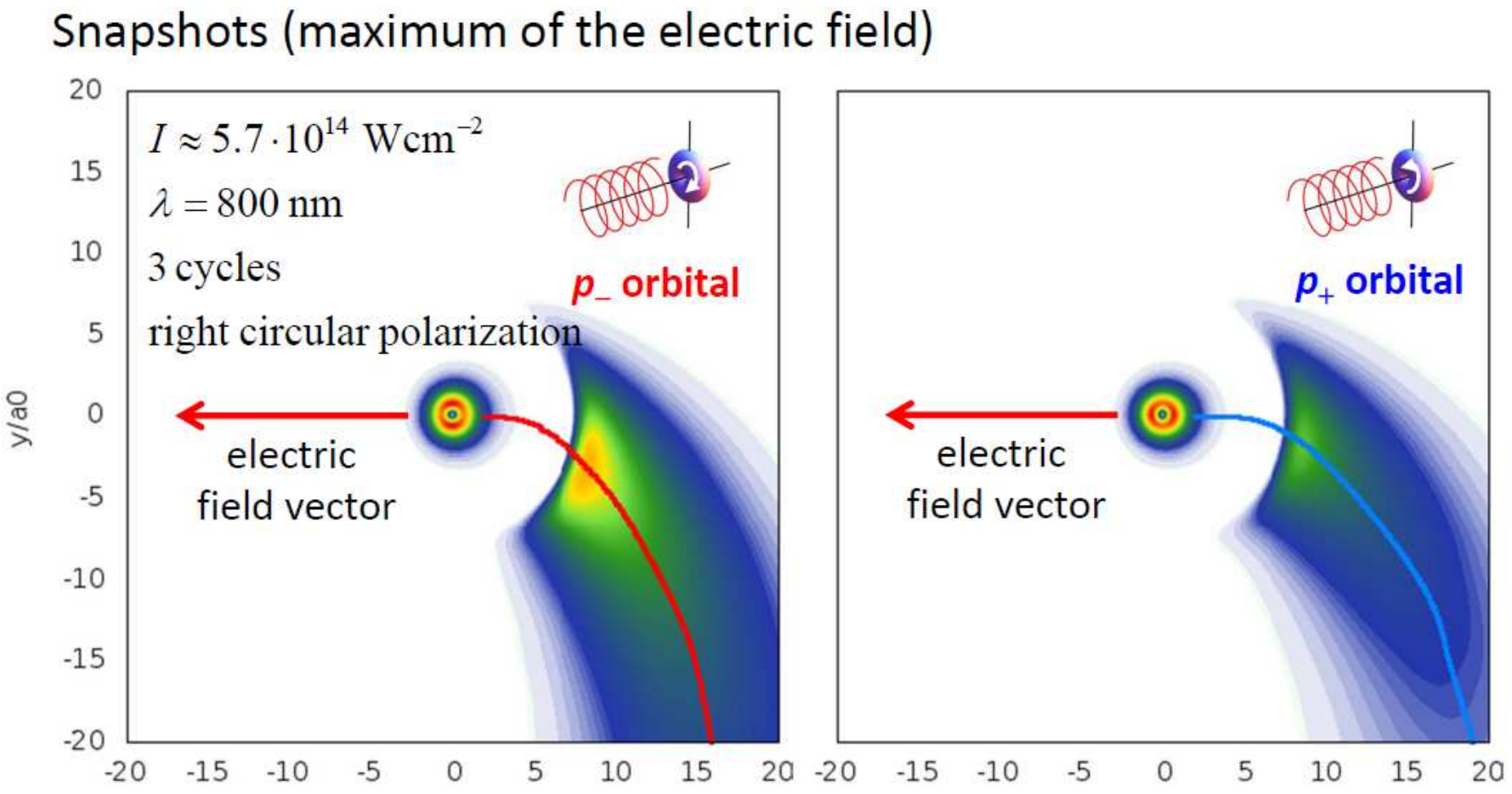

Agreement with PPT theory. *Also:* shifted emission angle!

m-dependence of atomic ionization

Ratio of ionization of p_- / p_+

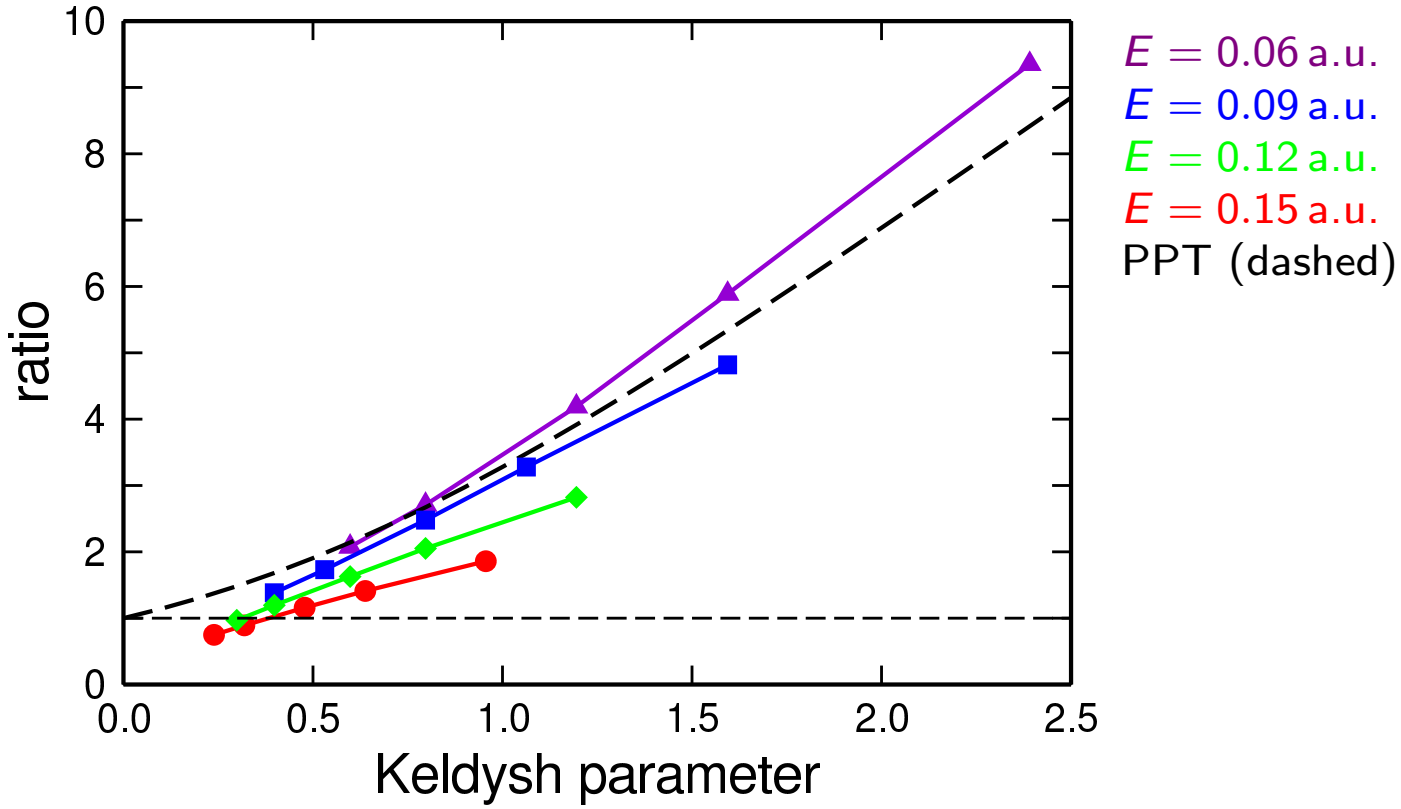

I. Barth and M.L., J. Phys. B, accepted

Agreement with PPT theory worsens for high intensity.

m-dependence of atomic ionization

Snaphots for very strong field $E = 0.15$ (1.6×10^{15} W/cm^2)

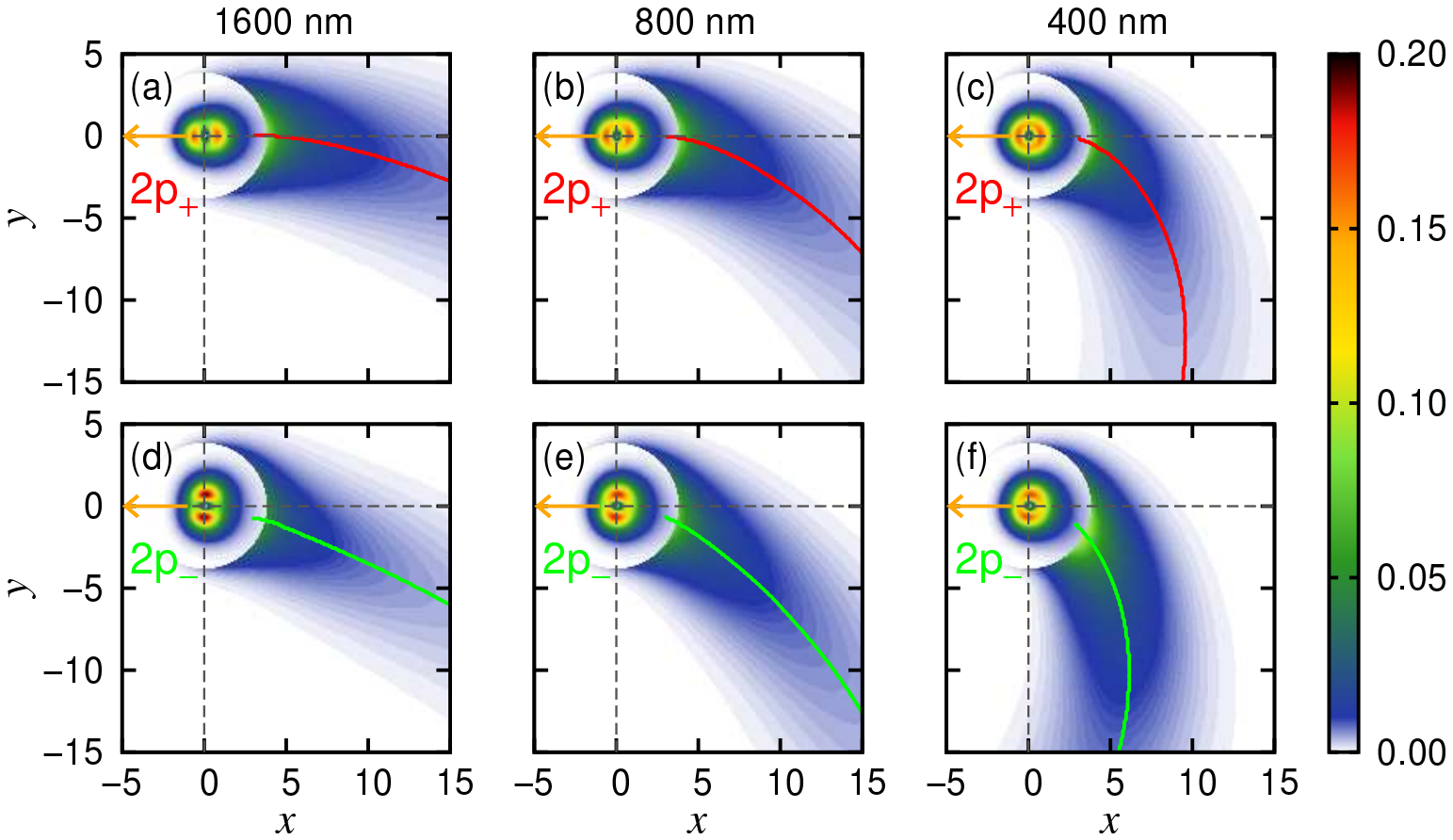

I. Barth and M.L., J. Phys. B, accepted

m-states changed into orbitals aligned parallel / perpendicular to instantaneous field [see also Mauger/Bandrauk, arXiv:1406.0105 (2014)]

m-dependence of atomic ionization

Three-state Floquet model for coupled s, p_-, p_+ states:

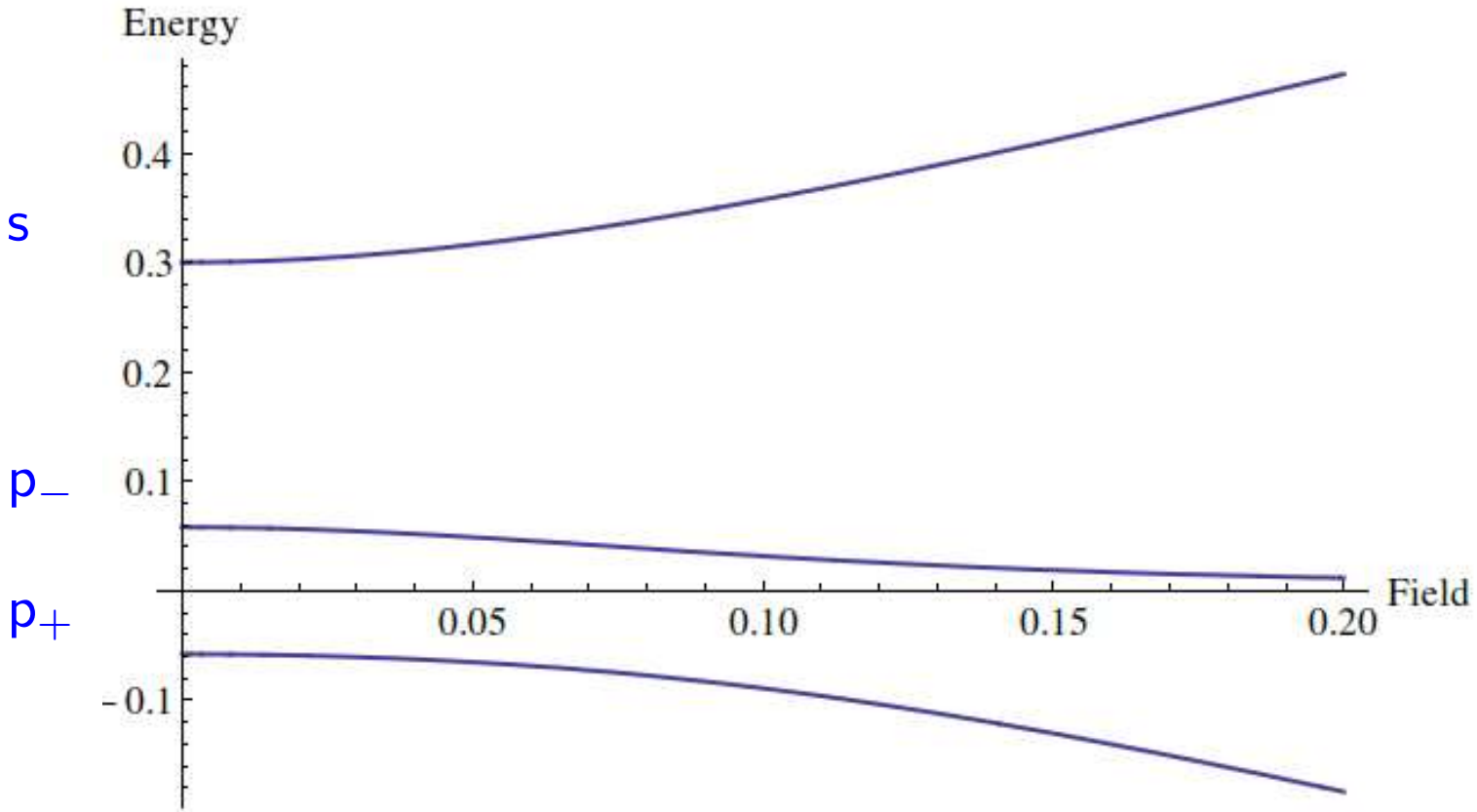

Evolution from $\{p_+, p_-, s\}$ to $\{p_{||}, p\perp, s\}$ dressed states.

$\rightarrow$ Preferential ionization of $p_{||}$,
suppressed ionization of $p\perp$ due to nodal plane.

Conclusions

- Transverse momentum width is measure of the instantaneous field and sensitive to the electronic structure. $\rightarrow$ Molecular imaging
- Born approximation/strong-field approximation for chiral molecules yields realistic photoelectron chiral dichroism, but is not quantitative.
- m-dependence of strong-field ionization in TDSE agrees with analytical theory at low intensity/high frequency (preferred ionization of counter-rotating electrons.) Deviations at high intensity/low frequency due to co-rotating dressed states.